Journal of Molecular Structure 1254 (2022) 132318

Contents lists available at ScienceDirect

Journal of Molecular Structure

journal homepage: www.elsevier.com/locate/molstr

Synthesis of diaryl urea derivatives and evaluation of their antiproliferative activities in colon adenocarcinoma

Muhammed Gömeç[a], Fatih Yulak[b], Hayreddin Gezegen[c], Mustafa Özkaraca[d], Koray Sayin[e,*], Hilmi Ataseven[f]

[a] Department of General Surgery, Faculty of Medicine, Cumhuriyet University, Sivas, Turkey
[b] Department of Physiology, Faculty of Medicine, Cumhuriyet University, Sivas, Turkey
[c] Department of Nutrition and Dietetics, Faculty of Health Sciences, Cumhuriyet University, Sivas, Turkey
[d] Department of Pathogy, Faculty of Veterinary, Cumhuriyet University, Sivas, Turkey
[e] Department of Chemistry, Faculty of Science, Cumhuriyet University, Sivas, Turkey
[f] Department of Gastroenterology, Faculty of Medicine, Cumhuriyet University, Sivas, Turkey

ARTICLE INFO

Article history:
Received 7 November 2021
Revised 17 December 2021
Accepted 29 December 2021
Available online 3 January 2022

Keywords:
Synthesis
Anticancer
Colon cancer
Diaryl urea
In silico

ABSTRACT

Colon cancer is one of the leading causes of cancer-related deaths today. Serious research for ideal chemotherapy continues today. In this context, newly synthesized molecules have an essential role in cancer treatment research. The effects of 5 diaryl urea derivatives synthesized within the scope of this study on the HT-29 colon cancer cell line were investigated for the first time in the literature by *in-silico* and *in-vitro* methods. Among the five compounds produced in the first stage of the study, DAU5 was found to have a cytotoxic effect on HT-29. However, it was determined that it did not show a serious cytotoxic effect on L929 (healthy fibroblast cell line) at the same doses. The efficacy of DAU5 was evaluated for expression of LC3B, an indicator of autophagy, and 8-OHdG, an indicator of oxidative stress-DNA damage. LC3B and 8-OHdG expression were lower in the DAU5 treatment group than in the control group. As a result, it was seen that DAU5, a diaryl urea derivative compound we synthesized in this study, has the potential to be a chemotherapeutic agent against colon cancer. However, our study needs to be supported by *in vivo* and clinical studies.

1. Introduction

Cancer is a pathological condition that occurs in the genetic and developmental process due to excessive proliferation of cells and loss of apoptosis functions. Colon cancer is a severe problem affecting both women and men, and according to the World Health Organization data, it is the third most common cause of cancer-related deaths [1]. Therefore, colon cancer continues to pose a severe public health problem. In addition to genetic factors, diet, smoking and alcohol habits, and inflammatory bowel disease play a role in its pathogenesis. Colon cancers can spread by invasion, lymphatic and hematological ways. Approximately 50% of colorectal cancers are complicated by metastases. However, only 10–20% of patients with liver metastases are resectable at presentation [2,3].

In addition to surgical interventions in the fight against cancer, radiotherapy and chemotherapy are frequently used treatment methods. In the treatment of colon cancer, chemotherapy is used for three main purposes: adjuvant, neoadjuvant, and palliative. When using adjuvant chemotherapy to prevent recurrence and distant metastasis after curative surgical resection, Neoadjuvant chemotherapy can also be applied to make unresectable masses resectable. Palliative chemotherapy is used in advanced tumors. As can be understood from all these usage areas, the place of chemotherapy in cancer treatment is gaining serious importance. It is known that the survival of colon cancer patients increases with regional or systemic chemotherapy [2]. For this reason, research on chemotherapeutics continues unabated. In these researches, studies including synthesis of new compounds and examination of bioactive potentials of these synthesized compounds make essential contributions to the discovery of new cancer drugs [4].

Diaryl urea-containing sulfonylureas have attracted the attention of researchers with their antibacterial [5], antifungal [6], and antimalarial properties as well as antitumor [7–11] properties. Regorafenib, a pyridine-based biphenyl urea derivative, inhibits VEGFR-1/3, PDGFRb, FGFR1, and Tie-2. Regorafenib is approved for use in the treatment of metastatic colorectal cancer. The antitumor effect of regorafenib is thought to be mediated by the induction of

* Corresponding author.
E-mail address: ksayin@cumhuriyet.edu.tr (K. Sayin).

https://doi.org/10.1016/j.molstruc.2021.132318
0022-2860/

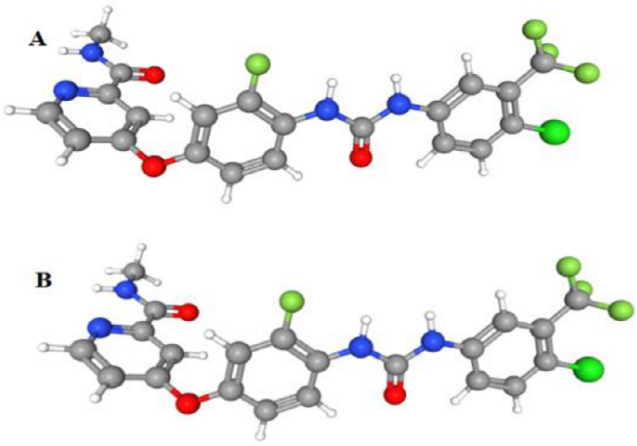

Fig.1. Chemical Structure of regorafenib(A) and sorafenib(B).

apoptosis and its antiangiogenic and antiproliferative effects [12–15]. Sorafenib is another urea-containing compound used in colorectal, hepatocellular, and kidney cancers [16] Fig. 1.

Autophagy plays a vital role in the regulation of protein homeostasis. It is a destructive intracellular system and contributes to the cell's survival by activating when the cell is exposed to metabolic stress [17]. Furthermore, recent studies have shown that some therapeutic agents can induce anticancer activities in line with autophagy-targeted strategies [18]. For example, studies have shown that cancer cells tend to increase autophagy as a protective mechanism to protect themselves from apoptosis activated by the effect of chemotherapeutic agents and radiotherapy treatments [19]. Various molecular and cellular signaling pathways such as LC3 (light chain), ATG5/ATG7 (autophagy-related protein 57), mTOR (mammalian target of rapamycin), reactive oxygen species (ROS), and Beclin-1 are actively involved in the regulation of autophagy [20]. Therefore, LC3B protein, which is one of the autophagy indicators, was chosen in our study.

Reactive oxygen species (ROS) are primarily produced endogenously due to metabolic events in living cells. Excess energy intake causes excessive production of nicotinamide adenine dinucleotide and superoxide anion in mitochondria. Increased ROS in the medium can readily attack proteins, lipids, and deoxyribonucleic acid (DNA) [21]. It has been suggested that DNA damage caused by oxidation leads to tumorigenesis. However, these damage mechanisms have not been explained [22]. 8-hydroxydeoxyguanosine (8-OHdG), the oxidatively modified product of proteins and DNA, is widely used as a marker for oxidative stress [23]. Therefore, in our study, the expression of 8-OHdG, which is both an indicator of oxidative stress and an indicator of DNA damage, was studied.

In the light of all these studies, besides many different effects of diaryl urea derivative syntheses, their anticancer properties come to the fore. Anticancer effects of diaryl urea derivatives have been demonstrated by many different mechanisms. In our study, five diaryl urea derivative molecules were synthesized. The effects of these synthesis products on colon cancer cells were demonstrated for the first time by *in silico* and *in vitro* methods.

2. Materials and methods

2.1. Reagents

4′-Aminoacetophenone, phthalaldehyde, 4-(trifluoromethyl) phenyl isocyanate, 4-methoxyphenyl isocyanate, 3-Chloro-4-(trifluoromethyl)phenyl isocyanate, 3-Chloro-4-methylphenyl isocyanate, 1-naphthyl isocyanate, and solvents which are toluene, DMSO was purchased from Merck kGaA.

2.2. Instrumentation

IR spectra (4000–400 cm^{-1}) were obtained using IR spectra (ATR) and recorded on a Bruker Tensor II FT-IR spectrometer. Melting points were measured on an Electrothermal IA9100 apparatus. ^{1}H-NMR and ^{13}C-NMR spectra were recorded on a JEOL (400 MHz) JNM-ECZ400S/L1 NMR instrument in DMSO–d_6 at room temperature; δ in ppm relative to tetramethylsilane (TMS), with J in hertz (Hz). Agilent Technology Inc. of 1260 Infinity HPLC System was coupled with 6530 Q-TOF LC/MS detector and ZORBAX SB-C18 (2.1 × 50 mm, 1.8 µm) column. ^{1}H NMR, ^{13}C NMR, and Q-TOF LC/MS analyses of the compounds were carried out at the Advanced Technology Application and Research Center (CUTAM) of Sivas Cumhuriyet University.

2.3. Synthesis of diaryl urea (DAU) derivatives

Synthesized compounds were the diaryl urea derivatives and took place in two steps. The related diaryl urea derivatives were synthesized based on a published article [24]. Schematic illustration of the synthesis was represented in Table 1. Related isocyanate derivatives are added to the solution of 4-aminoacetophenone in toluene and refluxed for three h. Formed participates are filtered and dried. The obtained solid was re-crystallized in DMSO to purify.

1-{4-[(1,3-D*ihydro*-1-*oxo*-2H-*inden*-2-*ylidene*)-*hydroxymethyl*] phenyl}−3-[4-(*trifluoro methyl*)*phenyl*]urea (**DAU1**). Yellow solid. Yield 78%. M.p. 277 – 280 °C. IR (KBr): 3535, 3307, 3069, 2945, 2900, 1646, 1628, 1601, 1578, 1546, 1470, 1410, 1372, 1328, 1268, 1225, 1165, 1122, 1108, 1068, 1015, 883, 838, 742, 656. ^{1}H NMR (600 MHz, DMSO-D_6) keto-enol (41:59), enol tautomer: 15.41 (s, 1H, -OH); 9.26 (s, 1H, -NH-); 9.23 (s, 1H, -NH-); 7.97 (d, J = 8.1, 2H, ArH); 7.78 (d, J = 7.4, 1H, ArH); 7.67 – 7.63 (m, 8H, ArH); 7.48 (br. s, 1H, ArH); 4.03 (s, 2H, -CH_2-). ^{13}C NMR (151 MHz, DMSO) δ 194.7, 171.0, 152.4, 149.0, 143.3, 137.5, 133.8, 129.8 (2C), 127.9, 127.6, 126.5 (q, J = 3.6 Hz, 2C), 126.4, 124.9 (q, J = 262.8 Hz), 123.0, 122.6, 122.4, 118.5 (2C), 118.2 (2C), 109.1, 32.3. HPLC-TOF/MS: 439.1226 ($[M+H]^+$, $C_{24}H_{18}F_3N_2O_3^+$; calc. 439.1264).

1-{4-[(1,3-D*ihydro*-1-*oxo*-2*H*-*inden*-2-*ylidene*)*hydroxymethyl*] phenyl}-3-(4-methoxy phenyl)urea (**DAU2**). Yellow solid. Yield 80%. M.p. 277 – 280 °C. IR (KBr): 3493, 3408, 3289, 3045, 2938, 2900, 2833, 1595, 1549, 1510, 1467, 1406, 1371, 1299, 1230, 1173, 1029, 880, 829, 740, 656. ^{1}H-NMR (600 MHz, DMSO-D_6) keto-enol (42:58), enol tautomer: 15.41 (*s*, 1H, -OH); 9.22 (*s*, 1H, -NH-); 8.76 (*s*, 1H, -NH-); 8.02 (*d*, J = 7.4, 1H, ArH); 7.95 (*d*, J = 7.4, 2H, ArH); 7.68 – 7.60 (*m*, 4H, ArH); 7.50 – 7.47 (*m*, 1H, ArH); 7.37 (*d*, J = 8.2, 2H, ArH); 6.87 (*d*, J = 7.8, 2H, ArH); 4.03 (*s*, 2H, -CH_2-); 3.71 (*s*, 3H, –OCH_3). ^{13}C-NMR (151 MHz, DMSO-D_6): 194.6; 171.2; 155.1; 152.8; 149.0; 144.0; 137.5; 133.8; 132.7; 129.8 (2 C); 128.1; 127.3; 126.4; 123.0; 120.6 (2 C); 117.9 (2 C); 114.4 (2 C); 109.0; 55.6; 32.3. HPLC-TOF/MS: 401.1370 ($[M+H]^+$, $C_{24}H_{21}N_2O_4^+$; calc. 401.1496).

1-[4-*Chloro*-3-(*trifluoromethyl*)*phenyl*]−3-{4-[(1,3-*dihydro*-1-*oxo*-2H-*inden*-2-*ylidene*) *hydroxymethyl*]-phenyl}urea (**DAU3**). Yellow solid. Yield 84%. M.p. 180 – 183 °C. IR (KBr): 3535, 3360, 3266, 3239, 3184, 3102, 3065, 3003, 2897, 1707, 1620, 1604, 1552, 1515, 1483, 1469, 1376, 1326, 1306, 1260, 1204, 1180, 1122, 1113, 1028, 960, 840, 748, 731, 550. ^{1}H NMR (600 MHz, DMSO-D_6) keto-enol (40:60), enol tautomer: 15.38 (*s*, 1H, -OH); 9.29 (*s*, 1H, -NH-); 9.27 (*s*, 1H, -NH-); 8.10 (*br. s*, 1 H, ArH); 8.04 (*d*, J = 7.3, 1H, ArH); 7.97 (*d*, J = 7.4, 2H, ArH); 7.67 – 7.61 (*m*, 6H, ArH); 7.51 – 7.47 (*m*, 1H, ArH); 4.04 (*s*, 2H, -CH_2-). ^{13}C NMR (151 MHz, DMSO-D_6): 194.7; 171.0; 152.5; 149.1; 143.2; 139.4; 139.3; 137.5; 132.4; 131.5; 129.8 (2 C); 127.2; 126.4; 124.1; 123.7; 123.1 (2 C);

Table 1
Synthesis route and Ar group is synthesized compounds.

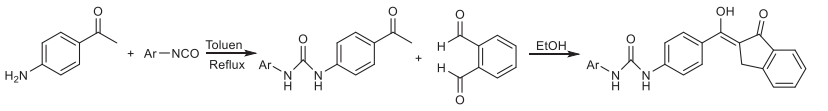

Compound	Ar
DAU1	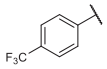
DAU2	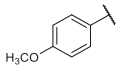
DAU3	
DAU4	
DAU5	

118.4 (2 C); 117.4 (q, J = 6.5); 109.1; 32.31. HPLC-TOF/MS: 473.0750 ($[M+H]^+$, $C_{24}H_{17}ClF_3N_2O_3^+$; calc. 473.0874).

1-(3–chloro-4-methylphenyl)–3-(4-(hydroxy(1-oxo-1,3-dihydro-2H-inden-2-ylidene) methyl) phenyl)urea (**DAU4**). Yellow solid. Yield 73%. M.p. 222 – 225 °C. IR (KBr): 3448, 3289, 3094, 3044, 2983, 1637, 1583, 1541, 1498, 1406, 1371, 1303, 1221, 1169, 1114, 1091, 1049, 994, 882, 837, 789, 740, 655, 549, 482. ^{1}H NMR (600 MHz, DMSO-D_6) keto-enol (41:59), enol tautomer: 15.52 (*s*, 1H, -OH); 9.16 (*s*, 1H, -NH-); 8.89 (*s*, 1H, -NH-); 8.03 (*d*, J = 7.2, 1H, ArH); 7.96 (*d*, J = 7.4, 2H, ArH); 7.69 (*br. s*, 1H, ArH); 7.66 – 7.62 (*m*, 4H, ArH); 7.50 – 7.46 (*m*, 1H, ArH); 7.24 (*d*, J = 8.2, 1H, ArH); 7.22 – 7.18 (*m*, 1H, ArH); 4.03 (*s*, 2H, -CH_2-), 2.25 (*s*, 3H, -CH_3). ^{13}C NMR (151 MHz, DMSO-D_6): 194.6; 171.1; 152.5; 149.0; 143.5; 138.9; 137.5; 133.8; 131.6; 130.2; 129.8 (2 C); 129.1; 128.1; 127.2; 126.4; 123.0; 118.1 (2 C); 117.6 (2 C); 109.1; 32.34; 19.28. HPLC-TOF/MS: 419.1117 ($[M+H]^+$, $C_{24}H_{20}ClN_2O_3^+$; calc. 419.1157).

1-{4-[(1,3-*Dihydro*-1-*oxo*-2H-*inden*-2-*ylidene*)-*hydroxymethyl*] phenyl}–3-naphthalen-1-ylurea (**DAU5**). Yellow solid. Yield 79%. M.p. 242 – 245 °C. IR (KBr): 3461, 3264, 3046, 3011, 2900, 1634, 1599, 1574, 1549, 1509, 1468, 1406, 1372, 1323, 1231, 1176, 1093, 1012, 881, 836, 783, 742, 659. ^{1}H NMR (600 MHz, DMSO-D_6) keto-enol (40:60), enol tautomer: 15.24 (*s*, 1H, -OH); 9.51 (*s*, 1H, -NH-); 8.90 (*s*, 1H, -NH-); 8.12 (*d*, J = 8.5, 1H, ArH); 8.06 (*d*, J = 7.2, 1H, ArH); 7.99 (*d*, J = 6.8, 2H, ArH); 7.93 (*d*, J = 8.1, 1H, ArH); 7.71 (*d*, J = 8.2, 2H, ArH); 7.67 – 7.63 (*m*, 4H, ArH); 7.59 (*t*, J = 7.5, 1H, ArH); 7.54 (*t*, J = 7.2, 1H, ArH); 7.48 (*d*, J = 6.8, 2H, ArH); 4.03 (*s*, 2H, -CH_2-). ^{13}C NMR (151 MHz, DMSO-D_6): 194.2; 171.1; 153.1; 149.0; 143.8; 137.5; 135.5; 134.1; 133.8; 131.6; 129.9; 128.8; 126.6; 126.3; 126.2 (2 C); 124.1; 123.9; 123.0; 121.8; 118.0 (2 C); 117.5; 109.0; 32.37. HPLC-TOF/MS: 421.1593 ($[M+H]^+$, $C_{27}H_{21}N_2O_3^+$; calc. 421.1547).

2.4. Computational chemistry

Gaussian software was used in the computational investigations [25,26]. The mentioned compounds were optimized at the M06–2X method with 6–31G(d) basis set in water. Additionally, polarizable Continuum Model (PCM) using the integral equation formalism variant (IEFPCM) was considered solute-solvent interactions. At the results of calculations, no imaginary frequency was observed. IR and NMR spectrum were calculated at the same level of theory. Some utilities such as ChemDraw were used in this study [27].

2.5. Molecular docking

The ground state structures of phenyl urea derivatives were obtained from computational calculations. In this stage, the Maestro program was used [28–31]. The ligand and target protein were prepared using LigPrep and Protein Preparation module, respectively. The receptor-binding domain of the target protein was defined using the Grid Generation module. pH was defined as 7 ± 2 in the whole calculations. Molecular docking calculations were performed using the Ligand Docking module.

2.6. Cell culture studies and development of HT-29 cells

In the present study, the human colon adenocarcinoma cell line (HT-29) obtained from the ATCC (American Type Culture Collection) was used. Cells were stored at 37 °C in a humidified atmosphere with 5% CO2, in 25 cm^2 flasks, 10% fetal bovine serum (FBS), 1% L-glutamine and 1% penicillin/streptomycin cultured in RPMI 1640 medium containing. Cells were passaged after reaching 80% density. After the third passage, the cell lines were prepared for study.

2.7. Cell viability assay

Colon cancer cell line HT-29 was used to evaluate the anticancer activity of **DAU1**-**DAU5** that we synthesized. TXT (2,3-bis-(2–methoxy-4-nitro-5- sulfophenyl)–5-[(*phenylamino*) *carbonyl*]–2H-tetrazolium hydroxide)(Biological Industries) colorimetric method was used for cell viability evaluation. Cells in the growth phase were seeded in a 96-well microplate at a density of 1 × 10^4 cells per well in RPMI 1640 culture medium (100 µL). After one day of incubation, the process was started. Five synthesis molecules were applied to the microplates at a dose of 20 µM. After 24 h of incubation, 40 µL of TXT reagent and DMEM mixture without phenol red (80 µL) was added to all wells, and the plates were incubated at 37 °C for 4 h. All experiments were repeated three times. Cell viability was compared with the drug-free control group. Optical density values were read on an ELISA reader at 450 nm (Thermo Fisher Scientific-Switzerland). The cell viability rate in the control group was accepted as 100%, and the results were obtained using the formula % Cell viability = (Concentration O.D./Control O.D.) X 100 were recorded. For ideal dose determination, the synthesis molecule with sufficient cytotoxic effect was

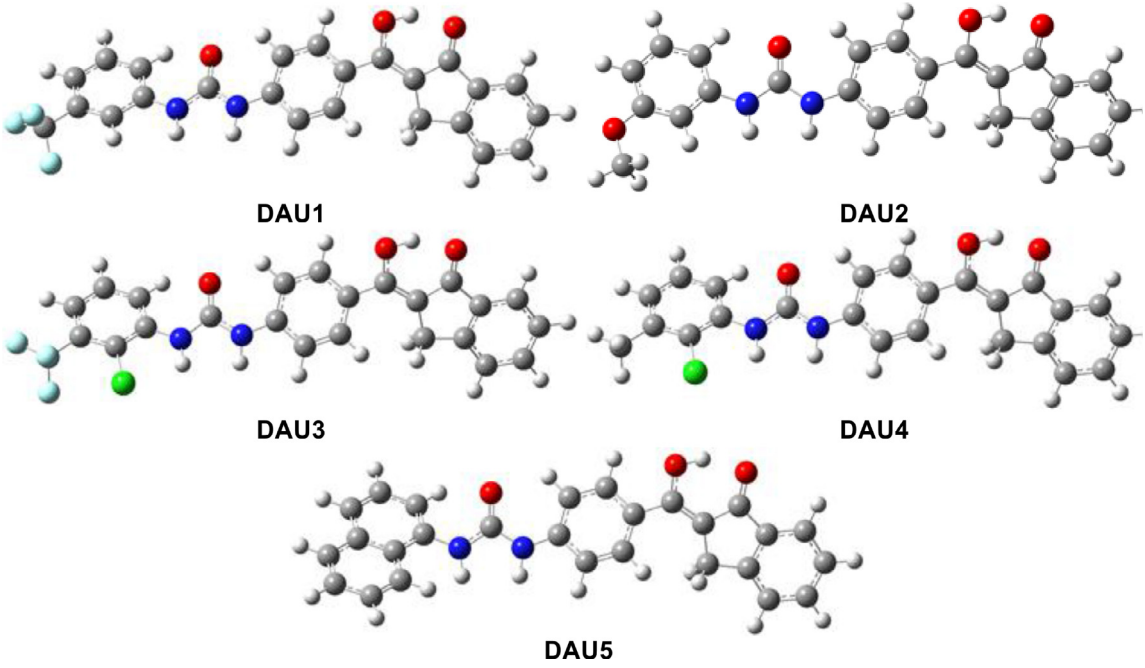

Fig. 2. Optimized structure of studied compounds.

applied to HT-29 again at different doses (80, 40, 20, 10.5 µM). The IC50 value (drug concentration causing 50% reduction in proliferation) was calculated using Graph Prism 7 software (GraphPad). Next, the possible cytotoxic effect on the healthy connective tissue cell line L929 was investigated to investigate the selectivity of the **DAU5** synthesis molecule to tumor cells. The active molecule was applied to the L929 cell line at doses of 80, 40, 20, 10, 5 µM.

2.8. Immunofluorescence examination

Cells were fixed with methanol for 5 min at −20 °C and washed with PBS. It was then incubated with PBS containing 0.1% Triton X-100 at room temperature for 15 min. After washing, it was incubated with PBS containing 2% BSA for 60 min. After rewashing, it was incubated overnight at +4 °C at 1/300 dilution with polyclonal anti LC3B (Abclonal, Catalog no. A7198) and monoclonal anti-8-OhDG (Santa Cruz, catalog no. sc-66,036) primary antibodies. Cells washed with PBS were incubated with goat anti-rabbit FITC and goat anti-mouse FITC secondary antibodies at a dilution ratio of 1/50 for 45 min at room temperature and in the dark. Finally, 4′,6-diamidino-2-phenylindole (DAPI) was dropped on the washed cells and examined under a fluorescence microscope. In the evaluation, positivity in cells in the whole area was evaluated semiquantitatively as absent (-), mild (+), moderate (++), and severe (+++).

2.9. Statistical analyses

The data analysis was done with the SPSS 23.0 package program. Results were expressed as mean ± standard deviation (SEM). Normally distributed data were evaluated using the one-way ANOVA Analysis of Variance Test. Data that did not show normal distribution were evaluated by applying the Kruskal-Wallis and Mann-Whitney U tests, non-parametric tests. The post hoc Tukey test was used to determine the differences between the experimental groups. Pathological data were analyzed with Student's *t*-test. The significance level was accepted as $P < 0.05$.

3. Results and discussion

3.1. Ground state structures

The studied diaryl urea derivatives are optimized at M06–2X/6–31G(d) level in the water. The optimized structures are represented in Fig. 2.

According to Fig. 1, the ground state structures are mainly planar for the mentioned compounds. The planarity of the compounds is mainly distorted by the benzene ring, which location is the left side of the compounds. Finally, there is an intramolecular hydrogen bond in each compound. This situation has gained extra stability to studied compounds.

3.2. Experimental and computational IR spectra

The experimental section gives the experimental section the positions of observed peaks in the IR spectra of studied diaryl urea derivatives (**DAU1** – **DAU5**) and their assignments based on extensive data available for related compounds. The IR spectra of mentioned compounds are given in Supplemental Material. Experimental and calculated frequencies of functional groups are given in Table 2.

3.3. NMR spectra

When the examined ^{1}H NMR spectra of the synthesized diaryl urea compounds (**DAU1-DAU5**), it is seen that the compounds are in the form of keto-enol at a ratio of approximately 40:60. In the ^{1}H NMR spectra of the synthesized diaryl urea compounds, it is seen that the prominent characteristic peaks are composed of the signals of enol proton, amide protons, and methylene protons in the structure. In the ^{1}H NMR spectra of **DAU1-DAU5**, the proton of the enol group (-OH) gave a broad singlet between δ 15.24–15.52 ppm. The amide protons of **DAU1-DAU5** gave a singlet between δ 9.16–9.51 ppm and 8.76–9.27 ppm, respectively. The methylene protons gave a singlet between δ 4.03–4.04 ppm.

In the ^{13}C NMR spectra of **DAU1-DAU5**, the carbonyl group in the indanon unit were resonated between δ 194.2–194.7 ppm, the

Table 2
Experimental and computational vibrational frequencies (cm^{-1}) of the related compounds.

Assignments	DAU1		DAU2		DAU3		DAU4		DAU5	
	Exp.	Calc.	Exp.	Calc.	Exp.	Calc.	Exp.	Calc.	Exp.	Calc.
ν_{OH}	3307	3200	3408	3198	3360	3212	3289	3199	3264	3196
ν_{NH}	3535	3628	3493	3637	3535	3633	3448	3622	3461	3645
$\nu_{CH\text{-}Aromatic}$	3069	3310–3212	3289–3045	3313–3211	3266–3065	3310–3225	3094–3044	3318–3212	3046–3011	3315–3212
$\nu_{CH\text{-}Aliphatic}$	2945, 2900	3117–3075	2938–2900	3203–3072	3003–2897	3116, 3078	2983	3183–3076	2900	3112
$\nu_{C=O}$	1646	1811	1595	1812	1707	1817	1637	1815	1634	1808

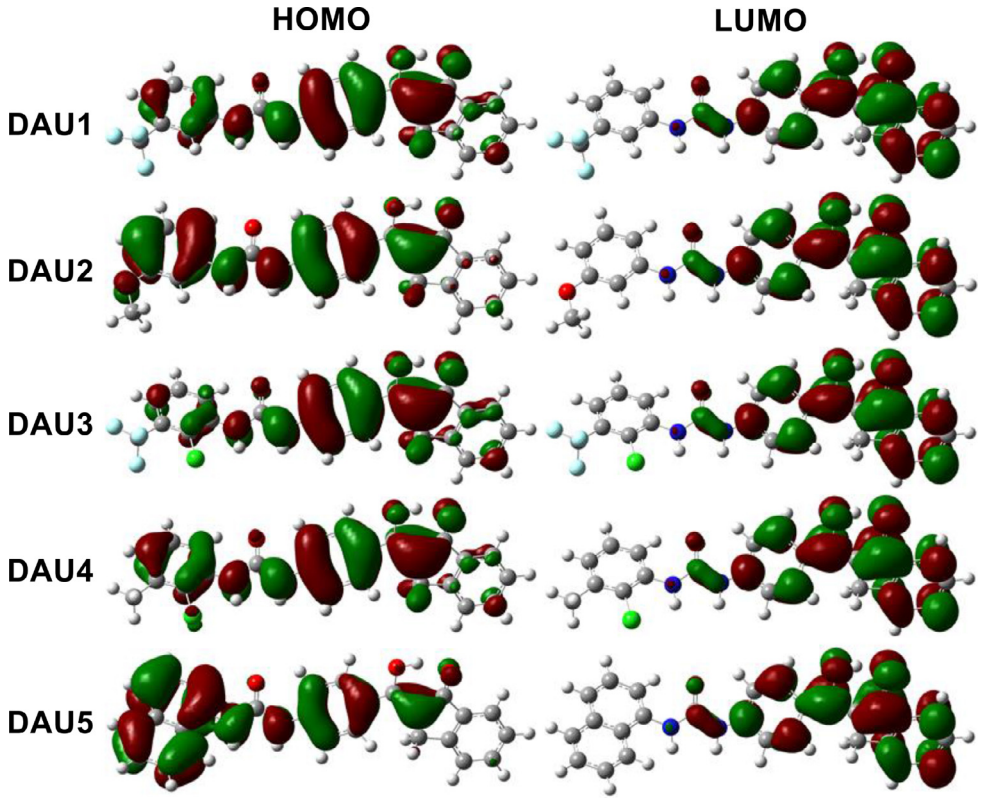

Fig. 3. Contour diagram of frontier molecular orbitals.

carbon atom of the amide group were resonated between δ 152.4–153.1 ppm. Among the two olefinic carbon atoms in the structure, the carbon of the enol group gave a signal between δ 171.0–171.2 ppm, while the other olefinic carbon atom gave a signal between δ 109.0–109.1 ppm. The signal, located at δ 32.3 ppm in the aliphatic region, comes from the carbon of the methylene unit in the structure.

3.4. Electronic properties

Electronic properties of the chemical are essential in determining the biological activity of compounds. For this aim, contour diagram of frontier molecular orbitals, which are the highest occupied molecular orbital (HOMO) and the lowest unoccupied molecular orbital (LUMO), and molecular electrostatic potential (MEP) map are calculated at the same level of theory. The contour diagrams of frontier molecular orbitals are represented in Fig. 3.

According to Fig. 3, electrons in HOMO are mainly delocalized on the whole structure. Especially, pi electrons are active in any interaction, especially on the benzene ring. On the other hand, pi electrons on the indanone are generally active. Furthermore, MEP maps of the related compounds are calculated and represented in Fig. 4.

According to Fig. 4, the environments of the heteroatoms are mainly reddish-yellow. Therefore, these atoms can be good potentials for the interactions. Furthermore, pi electrons on the benzene rings seem active due to the surface color. In general, the activity of **DAU5** seems more than the others due to the naphthalene group. Compared to other structures, pi electrons in naphthalene seem more active. However, the molecular reactivity in other regions except for the left side of the molecule seems to be the same.

3.5. Biological activity

AnticancerAnticancer activity of diaryl urea derivatives synthesized in the study was evaluated in the HT-29 colon cancer cell line. In the first step, the compounds were applied at a fixed concentration of 20 µM. Cell viability percentages were calculated after 24 h administration. Results below 60% were considered significant in the TXT viability test. The study was repeated three times, and the average cell viability; **DAU1** = 93.84% **DAU2** = 97.10% **DAU3** = 81.89% **DAU4** = 83.15% **DAU5** = 51.23% were detected. According to the statistical analysis, no lethal effect of **DAU1** and **DAU2** on HT-29 cells was observed. Although the cytotoxic effect of **DAU3** and **DAU4** in cells was statistically significant, it was observed that it was not at the desired level. Cell viability was 51,

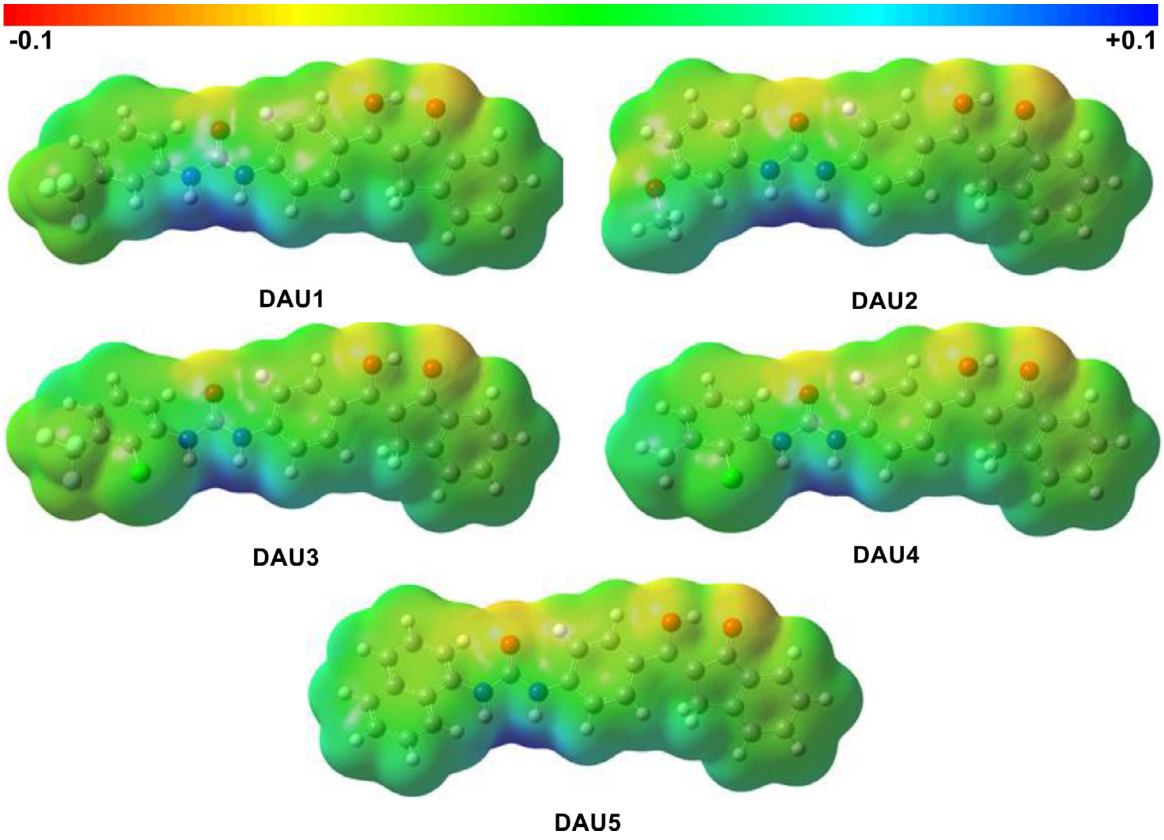

Fig. 4. MEP maps of the studied compounds.

Table 3
Results of Application of IF Molecules at a Dose of 20 µM to the HT-29 Cell Line.

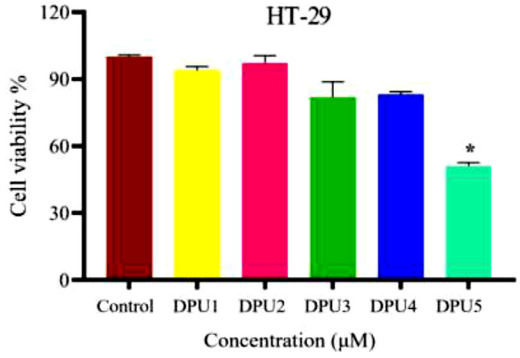

	n	*Mean±SD. Error*	*p*
Control	3	99.18 ± 0.84	–
DAU1	3	93.84 ± 1.71	$p = 0.854$
DAU2	3	97.10 ± 3.43	$p = 0{,}997$
DAU3	3	81.89 ± 6.87	$P < 0.05$
DAU4	3	83.15 ± 1.16	$p < 0.05$
DAU5	3	51.23 ± 1.22*	$p < 0.05$

* Cell viability <%55.

23% in **DAU5** (Table 3). Based on these results, the **DAU5** molecule was chosen as it caused cell viability to drop below 55% at a dose of 20 µM in the HT-29 cell line for further biological research.

In the present study, the next step was taken to determine the effective IC_{50} value of the **DAU5** molecule on HT-29. **DAU5** molecule was reapplied to HT-29 cell line at doses of 5 µM, 10 µM, 20 µM, 40 µM, 80 µM. Mean values in cell viability were obtained with TXT performed at the end of three repetitions. Cell viability was 97.22% at 5 µM, 85.00% at 10 µM, 50.83% at 20 µM, 36.94% at 40 µM, and 32.13% at 80 µM. The IC_{50} value was determined as 14.96 µM. In another phase of the study, the potential cytotoxicity of **DAU5** on the healthy fibroblast cell line L929 at the same doses was examined. At the end of three repetitions, mean values in cell viability were obtained with TXT. Cell viability was determined as 99.70% at 5 µM, 101.31% at 10 µM, 88.53% at 20 µM, 75.85% at 40 µM, and 48.49% at 80 µM (Table 5).

3.6. Molecular docking

Experimental and computational techniques can do determination of biological activity. As *in silico* analyses, molecular docking is the best option for this purpose. In this study, colon cancer is selected as a target for the studied compounds. In colon cancer, total 34 key targets have been explained by Zhang et al. in 2021 [https://doi.org/10.1186/s13040\055020\05500232\0559]. Especially, HSP90 has been reported as the most critical gene for colon cancer prevention. Molecular docking calculations are performed between studied compounds and target protein with PDB ID 4BQG. The x-y-z coordinate of the receptor-binding domain is 2.08–12.62–24.21. Molecular docking calculations are done. Docking score (DS), van der Waals interaction energy (E_{vdW}), Coulomb interaction energy (E_{Coul}), and total interaction energy (E_{Total}) of studied compounds are given in Table 5.

According to Table 3, there is only one active compound against the HSP90. The docking score is too low for the studied compound except for DAU5. It means that it is almost no key-lock compatibility, and studied compounds are inactive against the HSP90. Only DAU5 is active against HSP90. Additionally, the total interaction energy of DAU5 is the best in the studied compounds. The docking structure and interaction map of DAU5 are represented in Fig. 5.

Table 4
The efficacy of **DAU5** synthesis molecule in HT-29 and L929 cell lines at doses of 5 µM, 10 µM, 20 µM, 40 µM, 80 µM is shown in the table and graph.

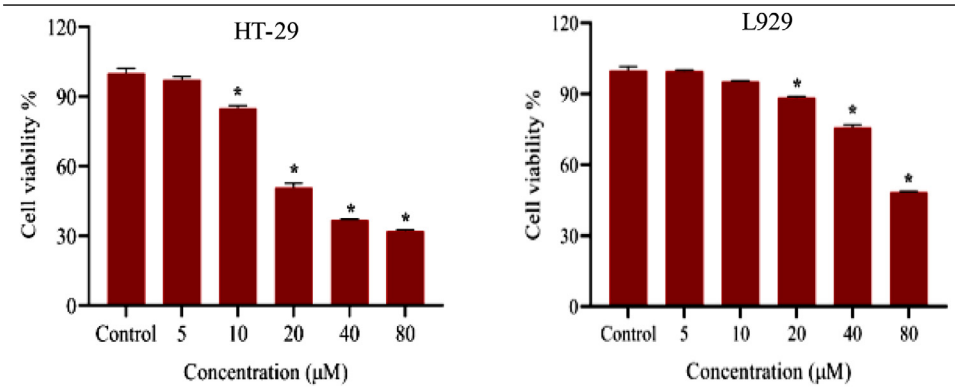

	HT-29			FIBROBLAST		
DAU5 Dose	*n*	*Mean±SD. Error*	*P*	*n*	*Mean±SD. Error*	*P*
Control	3	99.52 ± 2.13	–	3	98.52 ± 1.54	–
5 µM	3	97.22 ± 1.31	$p = 0.830$	3	99.70 ± 0.41	$p = 0.901$
10 µM	3	85.00 ± 1.12	$p < 0.05$	3	101.31 ± 0.29	$p = 0.223$
20 µM	3	50.83 ± 1.79	$p < 0.05$	3	88.53 ± 0.46	$p < 0.05$
40 µM	3	36.94 ± 0.32	$p < 0.05$	3	75.85 ± 1.05	$p < 0.05$
80 µM	3	32.13 ± 0.49	$p < 0.05$	3	48.49 ± 0.23	$p < 0.05$

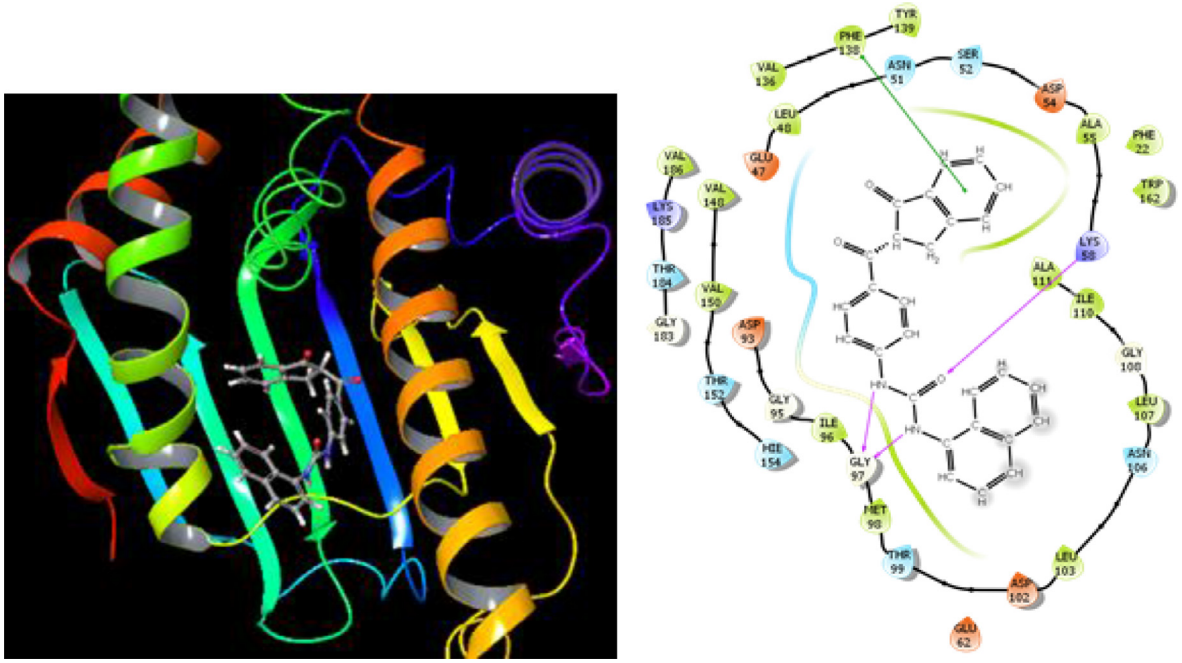

Fig. 5. The docking structure and interaction map between DAU5 and 4BQG.

Table 5
Molecular docking results.

Compound	DS[A]	E_{vdW}[a]	E_{Coul}[a]	E_{Total}[a]
DAU1	−2.74	−37.21	−9.19	−46.39
DAU2	−2.50	−37.93	−11.42	−49.35
DAU3	−1.34	−43.37	−6.29	−49.66
DAU4	−2.08	−45.80	−0.52	−46.32
DAU5	−6.95	−50.06	−4.64	−54.71

[a] in kcal/mol.

According to Fig. 5, pi-pi stacking, h-bond, polar interactions are the most critical interaction types. Furthermore, DAU5 is inhibited the HSP90 protein. It implies that DAU5 can be used in the prevention of colon cancer.

3.7. Immunofluorescence findings

It was determined that the difference between LC3B and 8-OhDG expressions in the cells stained in 6 different samples belonging to the control groups (CG) and **DAU5** groups was statistically significant. Tables of mentioned results are given in Supplementary Material.

While LC3B expression was mild in the CG, no significant expression was detected in the **DAU5** group. Moderate expression of 8-OhDG was detected in the CG but not in the **DAU5** group (Fig. 6).

Microtubule-associated protein LC3B, which controls mitochondrial quality against oxidative damage and is associated with cellular longevity, is an indicator of autophagy [32]. LC3B is a method to detect the amount of intracellular lysed products, the extent of

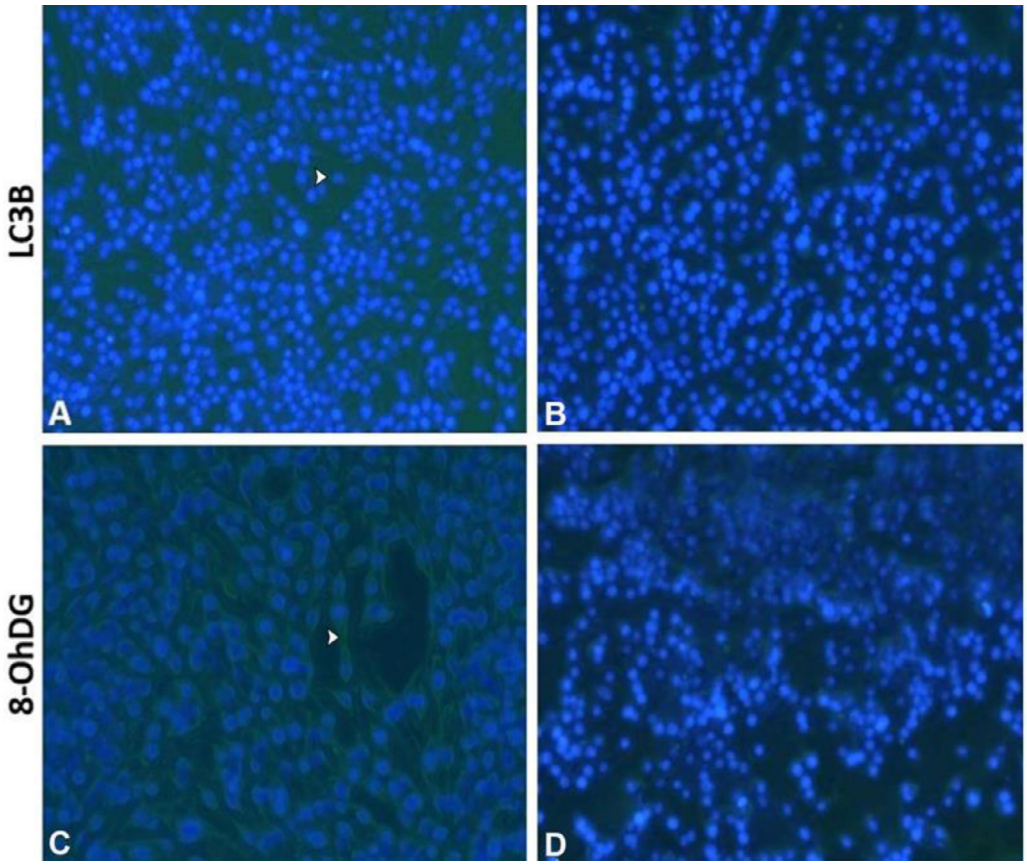

Fig 6. ***LC3B expression*** **A-** Mild level in CG (arrowhead), **B-** Negativity in **DAU5** group, ***8-OhDG expression*** **C-** Moderate level in the CG (arrowhead), **D-** Negativity in **DAU5** group. x20.

autophagosome formation, and the extent of autophagic activity. It has been reported that suppression of autophagy increases apoptosis, and therefore, drugs that suppress autophagy can provide therapeutic effects in cancer cells [33]. In our study, LC3B was studied as an indicator of autophagy. One of the biomarkers of ROS (Free oxygen radical) formation, oxidative stress, and DNA damage is 8-OHdG (8–hydroxy-2-deoxyguanosine) [34], resulting from free radical damage to guanine. In studies, high 8-OHdG levels have been associated with rat colon cancer, human breast cancer, and hepatocellular cancers [22,35–38]. Therefore, 8-OHdG expression was examined in our study.

In the light of this result, it was observed that **the DAU5** molecule significantly suppressed autophagy in HT-29 cells and showed the anticancer effect. In addition, it was observed that the expression of 8-OHdG decreased significantly in the treatment group in which the **DAU5** molecule was applied due to the activation of some possible repair mechanisms. All these results pathologically support the anticancer potential of the **DAU5** molecule, whose activity in the HT-29 colon cancer cell line was demonstrated by TXT colorimetric method.

4. Conclusion

Diaryl urea derivative compounds were analyzed. Molecular insertion was performed, and five urea derivative compounds were synthesized. Chemical analyzes of the synthesized compounds were completed. Then, the cytotoxic effects of the five diaryl urea derivative compounds we synthesized on the HT-29 colon cancer cell line were investigated. It was determined that the DAU5 compound had a cytotoxic effect on HT-29. In another stage of the study, it was observed that DAU5 did not have serious cytotoxicity on L929, a healthy fibroblast cell line, at doses that showed cytotoxic effects on colon cancer cells. This result proved that our compound has a more specific effect on colon cancer cells. After all these analyzes, the immunohistochemical examination was performed. When evaluated in terms of autophagy and DNA damage indicators, DAU5 has shown promising results in the treatment of colon cancer. This study, which is the first in the literature and supported by *in vitro* and *in silico* methods, needs to be supported by *in vivo* and clinical studies. As a result of our study, we see that DAU5 has the potential to contribute to the treatment of colon cancer.

Declaration of Competing Interest

The authors declare that they have no known competing financial interests or personal relationships that could have appeared to influence the work reported in this paper.

CRediT authorship contribution statement

Muhammed Gömeç: Formal analysis, Writing – review & editing. **Fatih Yulak:** Formal analysis. **Hayreddin Gezegen:** Writing – review & editing. **Mustafa Özkaraca:** Formal analysis. **Koray Sayin:** Formal analysis, Writing – review & editing. **Hilmi Ataseven:** Formal analysis, Writing – review & editing.

Acknowledgment

This work is supported by the Scientific Research Project Fund of Sivas Cumhuriyet University under the project numbers RGD-020 and F-2021–637. This research was made possible by TUBITAK

ULAKBIM, High Performance, and Grid Computing Center (TR-Grid e-Infrastructure). The authors are indebted to The Scientific and Technological Research Council of Turkey (Grant TUBITAK-114Z634) for financial support of this work.

Supplementary materials

Supplementary material associated with this article can be found, in the online version, at doi:10.1016/j.molstruc.2021.132318.

References

[1] R.C. Popescu, C. Tocia, C. Brînzan, G.C. Cozaru, M. Deacu, A. Dumitru, N. Leopa, A.F. Mitroi, A. Nicolau, E. Dumitru, Molecular profiling of the colon cancer in South-Eastern Romania: results from the MERCUR study, Medicine 100 (1) (2021) e24062.
[2] R. Adam, Chemotherapy and surgery: new perspectives on the treatment of unresectable liver metastases, Ann. Oncol. 14 (2003) ii13–ii16.
[3] J.Y. Kim, I.J. Park, H.R. Kim, D.K. Kim, J.L. Lee, Y.S. Yoon, C.W. Kim, S.B. Lim, J.B. Lee, C.S. Yu, J.C. Kim, Post-pulmonary metastasectomy prognosis after curative resection for colorectal cancer, Oncotarget 8 (22) (2017) 36566–36577.
[4] R.M. Bell, A review of complementary and alternative medicine practices among cancer survivors, Clin. J. Oncol. Nurs. 14 (3) (2010).
[5] L. Pan, Y. Jiang, Z. Liu, X.H. Liu, Z. Liu, G. Wang, Z.M. Li, D. Wang, Synthesis and evaluation of novel monosubstituted sulfonylurea derivatives as antituberculosis agents, Eur. J. Med. Chem. 50 (2012) 18–26.
[6] Y.T. Lee, C.J. Cui, E.W. Chow, N. Pue, T. Lonhienne, J.G. Wang, J.A. Fraser, L.W. Guddat, Sulfonylureas have antifungal activity and are potent inhibitors of Candida albicans acetohydroxyacid synthase, J. Med. Chem. 56 (1) (2013) 210–219.
[7] V.R. Avupati, R.P. Yejella, G. Guntuku, P. Gunta, Synthesis, characterization and *in vitro* biological evaluation of some novel diarylsulfonylureas as potential cytotoxic and antimicrobial agents, Bioorg. Med. Chem. Lett. 22 (2) (2012) 1031–1035.
[8] P. Rathore, S. Yaseen, S. Ovais, R. Bashir, R. Yaseen, A.D. Hameed, M. Samim, R. Gupta, F. Hussain, K. Javed, Synthesis and evaluation of some new pyrazoline substituted benzenesulfonylureas as potential antiproliferative agents, Bioorg. Med. Chem. Lett. 24 (7) (2014) 1685–1691.
[9] Z.J. Zhang, J. Tian, L.T. Wang, M.J. Wang, X. Nan, L. Yang, Y.Q. Liu, S.L. Morris-Nitschke, K.H. Lee, Design, synthesis and cytotoxic activity of novel sulfonylurea derivatives of podophyllotoxin, Bioorg. Med. Chem. 22 (1) (2014) 204–210.
[10] K. Szafrański, J. Sławiński, Synthesis of novel 1-(4-substituted pyridine-3-sulfonyl)-3-phenylureas with potential anticancer activity, Molecules 20 (7) (2015) 12029–12044.
[11] F.M. Sroor, A.M. Othman, M.A. Tantawy, K.F. Mahrous, M.E. El-Naggar, Synthesis, antimicrobial, anticancer and *in silico* studies of new urea derivatives, Bioorg. Chem. 112 (2021) 104953.
[12] L. Zhang, J. Yu, Role of apoptosis in colon cancer biology, therapy, and prevention, Curr. Colorectal Cancer Rep. 9 (4) (2013) 331–340.
[13] D. Chen, L. Wei, J. Yu, L. Zhang, Regorafenib inhibits colorectal tumor growth through PUMA-mediated apoptosis, Clin. Cancer Res. 20 (13) (2014) 3472–3484.
[14] M. Røed Skårderud, A. Polk, K. Kjeldgaard Vistisen, F.O. Larsen, D.L. Nielsen, Efficacy and safety of regorafenib in the treatment of metastatic colorectal cancer: a systematic review, Cancer Treat. Rev. 62 (2018) 61–73.
[15] X. Song, L. Shen, J. Tong, C. Kuang, S. Zeng, R.E. Schoen, J. Yu, H. Pei, L. Zhang, Mcl-1 inhibition overcomes intrinsic and acquired regorafenib resistance in colorectal cancer, Theranostics 10 (18) (2020) 8098–8110.
[16] N. Li, Y. Chen, H. Sun, T. Huang, T. Chen, Y. Jiang, Q. Yang, X. Yan, M. Wu, Decreasing acute toxicity and suppressing colorectal carcinoma using Sorafenib-loaded nanoparticles, Pharm. Dev. Technol. 25 (5) (2020) 556–565.
[17] J. Yang, C. Pi, G. Wang, Inhibition of PI3K/Akt/mTOR pathway by apigenin induces apoptosis and autophagy in hepatocellular carcinoma cells, Biomed. Pharmacother. 103 (2018) 699–707.
[18] J. Zhou, J. Yang, X. Fan, S. Hu, F. Zhou, J. Dong, S. Zhang, Y. Shang, X. Jiang, H. Guo, Chaperone-mediated autophagy regulates proliferation by targeting RND3 in gastric cancer, Autophagy 12 (3) (2016) 515–528.
[19] A. Apel, I. Herr, H. Schwarz, H.P. Rodemann, A. Mayer, Blocked autophagy sensitizes resistant carcinoma cells to radiation therapy, Cancer Res. 68 (5) (2008) 1485–1494.
[20] C.T. Chang, M. Korivi, H.C. Huang, V. Thiyagarajan, K.Y. Lin, P.J. Huang, J.Y. Liu, Y.C. Hseu, H.L. Yang, Inhibition of ROS production, autophagy or apoptosis signaling reversed the anticanceranticancer properties of Antrodia salmonea in triple-negative breast cancer (MDA-MB-231) cells, Food Chem. Toxicol. 103 (2017) 1–17.
[21] A.M. Pisoschi, A. Pop, F. Iordache, L. Stanca, G. Predoi, A.I. Serban, Oxidative stress mitigation by antioxidants - An overview on their chemistry and influences on health status, Eur. J. Med. Chem. 209 (2021) 112891.
[22] T. Sato, H. Takeda, S. Otake, J. Yokozawa, S. Nishise, S. Fujishima, T. Orii, T. Fukui, J. Takano, Y. Sasaki, K. Nagino, D. Iwano, T. Yaoita, S. Kawata, Increased plasma levels of 8-hydroxydeoxyguanosine are associated with development of colorectal tumors, J. Clin. Biochem. Nutr. 47 (1) (2010) 59–63.
[23] M. Graille, P. Wild, J.-J. Sauvain, M. Hemmendinger, I. Guseva Canu, N.B. Hopf, Urinary 8-OHdG as a biomarker for oxidative stress: a systematic literature review and meta-analysis, Int. J. Mol. Sci. 21 (11) (2020) 3743.
[24] H. Gezegen, C. Hepokur, U. Tutar, M. Ceylan, Synthesis and biological evaluation of novel 1-(4-(Hydroxy(1-oxo-1,3-dihydro-2H-inden-2-ylidene)methyl)phenyl)-3-phenylurea derivatives, Chem. Biodivers. 14 (10) (2017) e1700223.
[25] Gaussian 16, Revision C.01, M. J. Frisch, G. W. Trucks, H. B. Schlegel, G. E. Scuseria, M. A. Robb, J. R. Cheeseman, G. Scalmani, V. Barone, G. A. Petersson, H. Nakatsuji, X. Li, M. Caricato, A. V. Marenich, J. Bloino, B. G. Janesko, R. Gomperts, B. Mennucci, H. P. Hratchian, J. V. Ortiz, A. F. Izmaylov, J. L. Sonnenberg, D. Williams-Young, F. Ding, F. Lipparini, F. Egidi, J. Goings, B. Peng, A. Petrone, T. Henderson, D. Ranasinghe, V. G. Zakrzewski, J. Gao, N. Rega, G. Zheng, W. Liang, M. Hada, M. Ehara, K. Toyota, R. Fukuda, J. Hasegawa, M. Ishida, T. Nakajima, Y. Honda, O. Kitao, H. Nakai, T. Vreven, K. Throssell, J. A. Montgomery, Jr., J. E. Peralta, F. Ogliaro, M. J. Bearpark, J. J. Heyd, E. N. Brothers, K. N. Kudin, V. N. Staroverov, T. A. Keith, R. Kobayashi, J. Normand, K. Raghavachari, A. P. Rendell, J. C. Burant, S. S. Iyengar, J. Tomasi, M. Cossi, J. M. Millam, M. Klene, C. Adamo, R. Cammi, J. W. Ochterski, R. L. Martin, K. Morokuma, O. Farkas, J. B. Foresman, and D. J. Fox, Gaussian, Inc., Wallingford CT, 2016.
[26] GaussView, Version 6.1, Roy Dennington, Todd A. Keith, and John M. Millam, Semichem Inc., Shawnee Mission, KS, 2016.
[27] PerkinElmer, ChemBioDraw UltraVersion (15.1.0.144), Cambridge Soft, Waltham, MA, USA, 2016.
[28] Schrödinger Release 2021-4: LigPrep, Schrödinger, LLC, New York, NY, 2021.
[29] R.A. Friesner, R.B. Murphy, M.P. Repasky, L.L. Frye, J.R. Greenwood, T.A. Halgren, P.C. Sanschagrin, D.T. Mainz, Extra precision glide: docking and scoring incorporating a model of hydrophobic enclosure for protein-ligand complexes, J. Med. Chem. 49 (21) (2006) 6177–6196.
[30] Schrödinger Release 2021-4: Protein Preparation Wizard; Epik, Schrödinger, LLC, New York, NY, 2021; Impact, Schrödinger, LLC, New York, NY; Prime, Schrödinger, LLC, New York, NY, 2021.
[31] Schrödinger Release 2021-4: FEP+, Schrödinger, LLC, New York, NY, 2021.
[32] S. Mai, B. Muster, J. Bereiter-Hahn, M. Jendrach, Autophagy proteins LC3B, ATG5 and ATG12 participate in quality control after mitochondrial damage and influence lifespan, Autophagy 8 (1) (2012) 47–62.
[33] Y. Quan, H. Lei, W. Wahafu, Y. Liu, H. Ping, X. Zhang, Inhibition of autophagy enhances the anticanceranticancer effect of enzalutamide on bladder cancer, Biomed. Pharmacother. 120 (2019) 109490.
[34] A. Valavanidis, T. Vlachogianni, C. Fiotakis, 8-hydroxy-2′-deoxyguanosine (8-OHdG): a critical biomarker of oxidative stress and carcinogenesis, J. Environ. Sci. Health Part C 27 (2) (2009) 120–139.
[35] C. Ma-On, A. Sanpavat, P. Whongsiri, S. Suwannasin, N. Hirankarn, P. Tangkijvanich, C. Boone, Oxidative stress indicated by elevated expression of Nrf2 and 8-OHdG promotes hepatocellular carcinoma progression, Med. Oncol. 34 (4) (2017) 57.
[36] P.B. Ezhuthupurakkal, S. Ariraman, S. Arumugam, N. Subramaniyan, S.K. Muthuvel, P. Kumpati, B. Rajamani, T. Chinnasamy, Anticancer potential of ZnO nanoparticle-ferulic acid conjugate on Huh-7 and HepG2 cells and diethylnitrosamine induced hepatocellular cancer on Wistar albino rat, Nanomedicine: nanotechnology, Biol. Med. 14 (2) (2018) 415–428.
[37] Y. Dincer, S. Himmetoglu, T. Akcay, E.Y. Ersoy, K.N. Gunes, O. Tortum, Prognostic significances of oxidative DNA damage evaluated by 8-hydroxy-deoxyguanosine and antioxidant enzymes in patients undergoing resection of gastric and colon carcinoma, Neoplasma 54 (2) (2007) 131–136.
[38] A. Płachetka, B. Adamek, J.K. Strzelczyk, Ł. Krakowczyk, P. Migula, P. Nowak, A. Wiczkowski, 8-hydroxy-2′-deoxyguanosine in colorectal adenocarcinoma–is it a result of oxidative stress? Med. Sci. Monit. 19 (2013) 690 International medical journal of experimental and clinical research.